PROCEEDINGS OF SCIENCE

ONLINE ICRC 2021
THE ASTROPARTICLE PHYSICS CONFERENCE
Berlin | Germany
37th International Cosmic Ray Conference
12–23 July 2021

Time-Delay Measurements from Antarctic Neutron Monitor Stations Indicate Weak Spectral Changes during 27-day Variations

Pradiphat Muangha,[a,*] **David Ruffolo,**[a] **Alejandro Sáiz,**[a] **Chanoknan Banglieng,**[a,b] **Paul Evenson,**[c] **Surujhdeo Seunarine,**[d] **Suyeon Oh,**[e] **Jongil Jung,**[f] **Marc Duldig**[g] **and John Humble**[g]

[a] *Mahidol University, Department of Physics, Faculty of Science, Bangkok 10400, Thailand*
[b] *Rajamangala University of Technology Thanyaburi, Division of Physics, Faculty of Science and Technology, Pathum Thani 12110, Thailand*
[c] *University of Delaware, Department of Physics and Astronomy, Newark, DE 19716, USA*
[d] *University of Wisconsin River Falls, Department of Physics, River Falls, WI 54022, USA*
[e] *Chungnam National University, Department of Astronomy, Space Science and Geology, Daejeon 34134, South Korea*
[f] *Chonnam National University, Department of Earth Science Education, Gwangju 61186, South Korea*
[g] *University of Tasmania, School of Natural Sciences, Hobart, Tasmania 7001, Australia*
E-mail: fhoone@hotmail.com, david.ruf@mahidol.ac.th, alejandro.sai@mahidol.ac.th, evenson@udel.edu, surujhdeo.seunarine@uwrf.edu

Using neutron time-delay data from neutron monitors (NMs), we can extract the leader fraction, L, of neutron counts that do not follow a previous neutron count in the same counter tube due to the same cosmic ray shower. L is the inverse of the neutron multiplicity and serves as a proxy of the cosmic ray spectral index over the rigidity range of the NM response function. We have outfitted several Antarctic NMs with special electronics to collect neutron time delay distributions. We present a comparative analysis of L during two time periods: 1) during December 2015 to January 2017, for NMs at South Pole (SP), McMurdo (MC), and Jang Bogo (JB), and 2) during February 2020 to February 2021, for NMs at SP, JB, and Mawson (MA). To first order L varies in concert with the count rate C, reflecting unrolling of the Galactic cosmic ray (GCR) spectrum as part of solar modulation during the declining phase of solar cycle 24 and during solar minimum. However, during 27-day variations in C due to high-speed solar wind streams (HSSs) and corotating interaction regions (CIRs), L usually had a very weak variation. Our results indicate weak GeV-range GCR spectral variation due to HSSs and CIRs, relative to the flux variation, in contrast with the strong observed spectral variation due to solar modulation.

37th International Cosmic Ray Conference (ICRC 2021)
July 12th – 23rd, 2021
Online – Berlin, Germany

*Presenter

PoS(ICRC2021)1285

1. Introduction

Neutron monitors (NMs) are ground-based detectors of secondary particles produced in atmospheric cascades from primary cosmic ray ions. NMs consist of several proportional counters (mainly filled with BF_3 or ^{3}He gas), which are sensitive to the neutrons produced by the interaction of the secondary particles with a dense lead producer. Monitoring the count rate C provides information about variations of the cosmic ray flux entering at the top of the atmosphere due to the solar modulation, in particular the long term modulation (with the ∼11-year sunspot cycle and the ∼22-year solar magnetic cycle) as well as the short-term variations (the Forbush decreases from solar activity and the ∼27-day and daily variations related to the solar rotation and the Earth's rotation, respectively). In particular, 27-day variations relate to high-speed solar wind stream emitted from coronal hole regions at the Sun and corotating interaction regions (CIRs) in interplanetary space, which pass the Earth repeatedly in successive solar rotations [1–3].

Specialized electronics have been designed to record neutron time-delay histograms [e.g., 4, 5]. Previous work developed techniques to remove the effect of chance coincidences and extract the "leader fraction" L of neutron monitor counts that did not follow other counts in the same counter tube from the same cosmic ray shower [6–8]. This work mainly focuses on a comparative analysis of L during two time periods: 1) during December 2015 to January 2017, for NMs at South Pole (SP), McMurdo (MC), and Jang Bogo (JB), and 2) during February 2020 to February 2021, for NMs at SP, JB, and Mawson (MA). We observe 27-day variations in C much stronger than in L and examine the relationship between the 27-day GCR variations and heliospheric parameters.

2. Neutron monitor time-delay histograms

Using neutron time-delay data from a single station with specialized electronics, we can indicate variations in the cosmic-ray spectral index [6]. The South Pole NM (SP), at an altitude of 2828 m, has three 1NM64 detectors. The SP NM started using these electronics on one NM tube to record the time-delay histograms in 2013 December and the complete set of 3 counter tubes in 2015 March. For each of the three tubes, the electronics provided hourly time delay histograms with different time scales. For more details about the experimental determination of the time-delay histograms, we refer to [6]. At long time delays, the histogram has an exponential tail representing chance coincidences between two unrelated incoming secondary particles (mostly neutrons) while at short time delays the histogram is non-exponential, which can be attributed to temporally associated neutron counts that originated from the same primary cosmic ray.

Jang Bogo (JB) station, at latitude -74.6°N, longitude 164.2°E, and altitude 48 m, is located close to McMurdo (MC) station at latitude -77.9°N, longitude 166.6°E, and altitude 30 m, and received 5 NM tubes with these special electronics from MC in December, 2015 [9]. The MC station was closed in January 2017. Around January 2019, 12 NM tubes from MC arrived at JB, with special electronics on 6 tubes. Now JB has 11 NM tubes that can collect time delay histograms. During December 2015 to January 2017, MC station used these electronics on 6 NM tubes.

The NM at Mawson (MA) station, at latitude −67.6°N, longitude 62.8°E, and altitude 30 m, had such electronic firmware installed to start measuring time-delay histograms in early February, 2020 for 18 NM tubes.

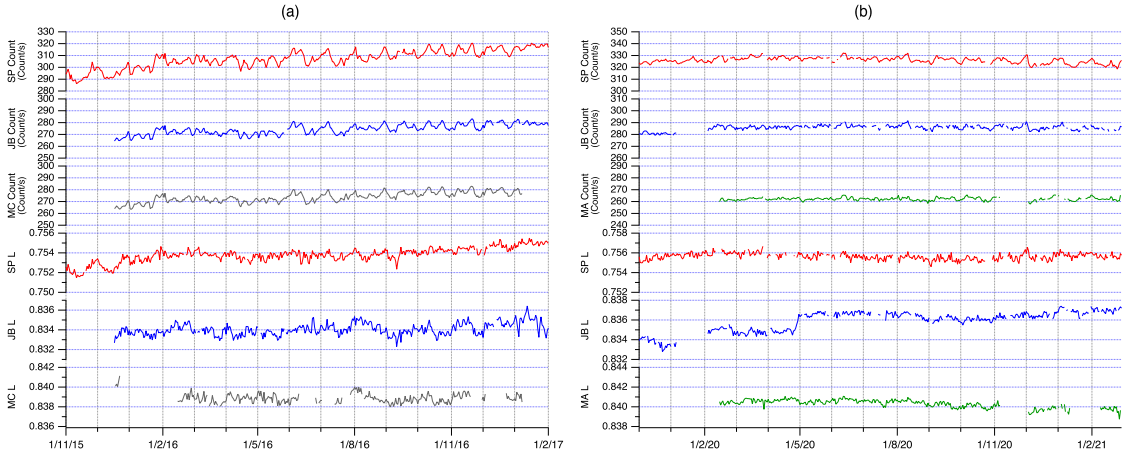

Figure 1: **(a)** Comparison of daily averaged count rates from 2015 December to 2017 February from the South Pole, Jang Bogo, and McMurdo NMs. Each NM count rate has the same trend. Variations in the leader fraction L indicate changes in the cosmic-ray spectrum. **(b)** Comparison of daily averaged count rates from 2020 February to 2021 February from the South Pole, Jang Bogo, and Mawson NMs.

The leader fraction L, defined as the fraction of neutron counts that did not follow a previous neutron count in the same tube from the same cosmic ray, is the inverse multiplicity and a proxy of the GCR spectral index above the cutoff. Referring to [6], it is possible to statistically remove the effect of chance coincidences to extract the leader fraction L from each time delay histogram, i.e., for each counter tube and each time interval.

When the secondary particles interact in the NM producer (mostly in the lead), a harder spectrum should lead to producing more neutrons with a greater multiplicity and a lower leader fraction. Therefore, a lower leader fraction is associated with a harder cosmic-ray spectrum with a lower spectral index [7]. [6] showed that the leader fraction at Doi Inthanon can indicate short-term spectral variations. Note that NM count rates are always corrected for pressure variation, and the leader fraction L has been found to vary with P as well. The pressure-corrected L for each counter tube is different, mainly due to its position and electronic dead time.

3. Observations

3.1 Comparative analysis of leader fraction

Here we present observed variations in L and the count rate C at the Antarctic NM stations SP, JB, MC, and MA. SP recorded the highest C, about 300 counts/s, and the lowest L, about 0.75 (Figure 1), because SP is at high altitude and the other stations are near sea level. Figure 1(a) presents data for the period of December 2015 to January 2017, when SP, JB, and MC simultaneously collected time delay histograms. JB and MC are well correlated and have similar values of C and L (about 270 counts/sec and 0.83, respectively) because these two stations are close to each other. Figure 1(b) shows C and L during February 2020 to February 2021, when SP, JB, and MA took time delay data over the same period. MA station has a higher L (about 0.84) and lower C (about 260 counts/sec). In Figure 1(a), NM count rates clearly show 27-day modulation while the leader fraction has little

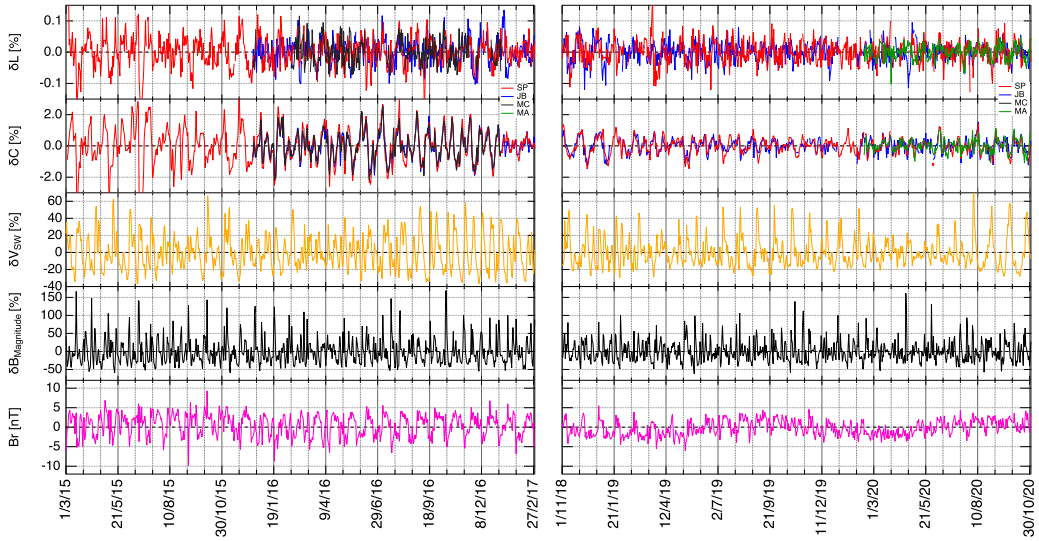

Figure 2: Daily NM count rate C, L, solar wind velocity, IMF magnitude as normalized and detrended over 27-day smoothing, and the daily IMF B_r component for March 2015 to February 2017 (left) and July 2018 to June 2020 (right).

variation, except in late 2015 when both the SP count rate and L showed strong 27-day variations. Around June 2016, SP, JB, and MC count rates clearly exhibited 27-day variations but L did not. In Figure 1(b), the 27-day variations are generally weaker. The jump in the JB leader fraction is due to changing the software version on April 29, 2020. Taking this into account, the variations in L and C are generally consistent among all these Antarctic NM stations.

3.2 Periodic variation of the GCR flux and spectral index and heliospheric parameters

We used data of the neutron monitors located at South Pole, Jang Bogo, McMurdo, and Mawson, which have geomagnetic cutoff rigidities of $R_c < 1$ GV, so the detector response is determined by an atmospheric cutoff at ~1 GV. The pressure-corrected data of the GCR count rate C and leader fraction L were detrended as $\delta \mathrm{I}[\%] = 100 \times (x_i - \bar{x})/\bar{x}$ to remove the longer-term variations in solar modulation, where x is the daily-averaged C or L and $\bar{x}$ the 27-d moving average. The detrended daily values are presented for the GCR count rate C and leader fraction L in Figure 2, along with some detrended solar wind (SW) parameters: the solar wind velocity, interplanetary magnetic field (IMF) magnitude, and the IMF Br component. These solar wind parameters were obtained from OMNI2 data (https://spdf.gsfc.nasa.gov/pub/data/omni/).

Thus Figure 2 illustrates the 27-day variations in GCR flux and spectral index and in solar wind parameters during March 2015 to February 2017 (left) and July 2018 to June 2020 (right). These detrended data show fluctuations about zero. Count rate C peaks occur mostly near the same times in all the cosmic ray rates, corresponding with minima in the solar wind speed, which occur at magnetic sector crossings in the slow speed wind (as indicated by B_r). There are strong two peaks in the SW speed (middle panel) during late 2016 corresponding with two peaks in C but no clear variation in L (mostly one peak with weak variation). The 27-day variations in L are mostly similar in shape to C but are observed to be much weaker. In the right panel, both C and L exhibit weaker

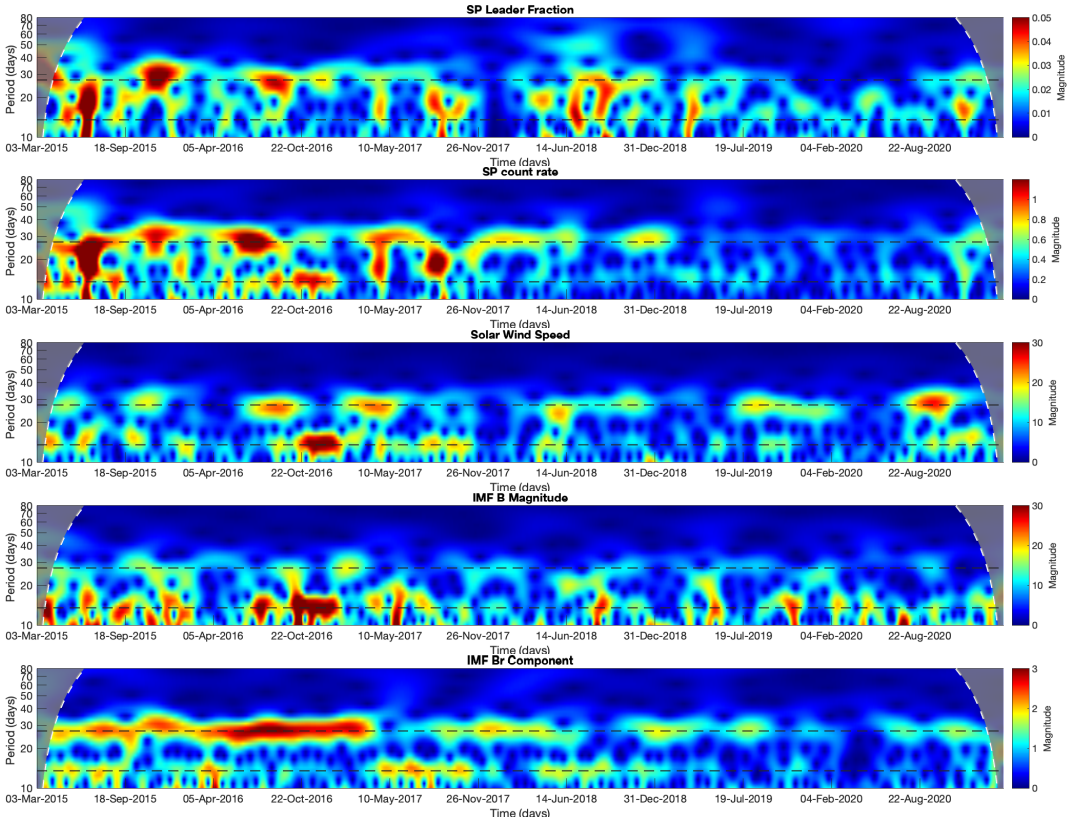

Figure 3: Wavelet analysis of daily SP L, C, solar wind speed, IMF magnitude, and IMF B_r component for March 2015 to February 2021. White dashed line corresponds to the 95% confidence level. Horizontal black dashed lines for each panel correspond to the periods of 27 days and 13.5 days, respectively.

27-day variation than in the left panel, in association with weaker variation in the solar wind speed and interplanetary magnetic field (IMF).

To examine the temporal changes of the periodic variation associated with the Suns rotation, in Figure 3 we present results of Morlet wavelet analysis of the South Pole count rate C [%], South Pole leader fraction L [%], IMF magnitude B [nT], and IMF B_r component [nT]. The count rate C mostly exhibits two significant signals with periodicities of ~27 days and ~13.5 days that are mostly similar those of the solar wind velocity. L seems to be associated with C in ~ 27-day periodicity but weak in the periodicity of the 2nd harmonic (~13.5 days). For example, during late 2016, SW and C data show a strong signal at the half period of solar rotation. This implies that two nearly opposite regions of the near-equatorial solar surface produced faster solar wind and affected cosmic ray count rates, but only one of them affected the cosmic ray spectrum. The other one apparently does not because L varies with the full period rather than the half period. Over the same time period, the IMF B_r component exhibited strong variation with a 27-day period and B clearly exhibited the ~13.5-day period, which is characteristic of a two-sector structure.

3.3 Characteristic features of 27-day variations in GCR flux and spectral index

We consider the relationship between the detrended 27-day variations in C (indicating GCR flux variation) and L (indicating GCR spectral index variation) vs. solar wind speed and IMF

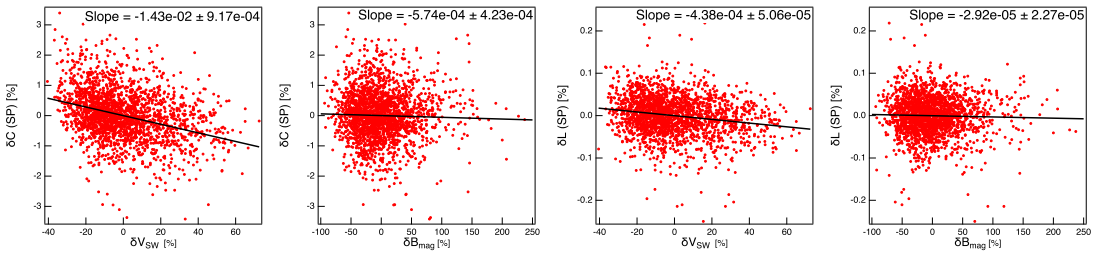

Figure 4: Percent differences between the daily-averaged values and the 27-day running averages of the South Pole neutron monitor count rate C and leader fraction L versus the analogous percent differences in the solar wind speed and in the magnetic field magnitude during the period March 2015 - February 2021.

magnitude. Results show that C and L variations are significantly correlated with the solar wind speed variation, in all cases, but not with the magnetic field magnitude variation, in any cases, as shown in Figure 4 for the example of the SP station. We define a significant correlation from a linear fit coefficient of the detrended of C or L versus the detrended V_{SW} or B greater than twice its uncertainty. The correlation coefficients as shown in Table 1 imply that the time behavior in the period of 27-day variation of GCR flux and spectral index are more affected by solar wind speed variation. Note that we use data from December 2015 - February 2021 for SP and JB, December 2015 - January 2017 for MC, and February 2020 - February 2021 for MA.

Table 1: The linear coefficients of 27-day variations in count rate and leader fraction versus solar wind speed and magnetic field magnitude.

	NM station	Solar Wind Speed	Magnetic Field Magnitude
Count Rate	South Pole	−1.43E − 02 ± 9.17E − 04	−5.74E − 04 ± 4.23E − 04
	Jang Bogo	−9.99E − 03 ± 8.07E − 04	−3.15E − 04 ± 3.64E − 04
	McMurdo	−2.13E − 02 ± 1.89E − 03	−7.06E − 05 ± 1.02E − 03
	Mawson	−5.43E − 03 ± 1.29E − 03	8.55E − 04 ± 5.39E − 04
Leader Fraction	South Pole	−4.38E − 04 ± 5.06E − 05	−2.92E − 05 ± 2.27E − 05
	Jang Bogo	−2.29E − 04 ± 7.05E − 05	−1.60E − 05 ± 3.05E − 05
	McMurdo	−4.68E − 04 ± 1.13E − 04	3.12E − 06 ± 5.97E − 05
	Mawson	−2.58E − 04 ± 0.80E − 04	1.74E − 05 ± 3.38E − 05

In Figure 5 we consider superposed epoch analyses of the 27-day variation of the GCR spectral index, flux, solar wind velocity and magnetic field during January 2016 January 2017 [corresponding to Bartels rotations (BR) 2489-2502; Fig. 2 (a)] and February 2020 February 2021 [BR 2545-2558; Fig. 2 (b)]. For each time period, we plot the average data over the 14 BRs. The two decreases in the solar wind speed per solar rotation clearly correlate with enhancements in C and L. The peak-to-peak percent change in L is ≈ 0.035 that of C. In comparison, for the solar modulation from late March, 2015 to mid-April, 2018 as reported in Figure 5 of [8], the ratio of fractional changes in L to C is ≈ 0.046. Thus even for the time period of January 2016 - January 2017, when 27-day variations in L were particularly clear, the spectral variation was relatively weak compared with that for modulation with the sunspot cycle.

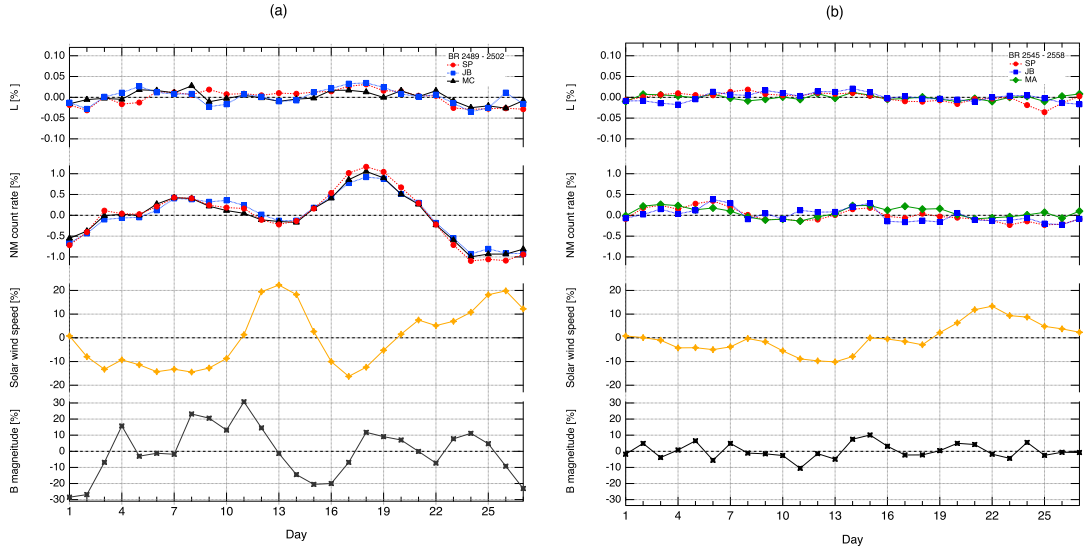

Figure 5: Superposed epoch analysis of L, C, V_{SW}, and B over the 27-day solar rotation period (Bartels rotation, BR), showing mean values over 14 BRs during **(a)** January 2016 - January 2017 (BR 2489 to 2502) and **(b)** February 2020 - February 2021 (BR 2545 to 2558).

Figure 6 shows that the amplitude of the 27-day variation in C was very similar for different NM stations. For L, the amplitude profiles were qualitatively similar for different stations, though different in detail. The SP data indicate a large amplitude of the 27-day GCR variations in the period of November-December 2015; for these BRs the ratio of fraction changes in L and C is similar to that for solar modulation. The 27-day variations of both C and L were strong during 2015-2016 but continuously weak during 2019-2020. This variation mainly corresponded to CIR and sector activity in the solar wind, in terms of the SW speed and IMF B_r component, respectively. The B_r component had periodic variations during 2016 that were stronger and more stable than those of other variables. In late 2020, the strong 27-day variation in SW speed started earlier and heralded a minor increase in the 27-day variation in C and L.

4. Acknowledgments

We acknowledge logistical support from Australias Antarctic Program for operating the Mawson NM and support from the National Astronomical Research Institute of Thailand and grant RTA6280002 from Thailand Science Research and Innovation.

References

[1] W. H. Fonger, *Cosmic Radiation Intensity-Time Variations and Their Origin. II. Energy Dependence of 27-Day Variations*, *Phys. Rev.*, 91, 351, 1953.

[2] R. Modzelewska and M.V. Alania, *The 27-Day Cosmic Ray Intensity Variations During Solar Minimum 23/24*, *Solar Physics*, 286, 593607, 2013.

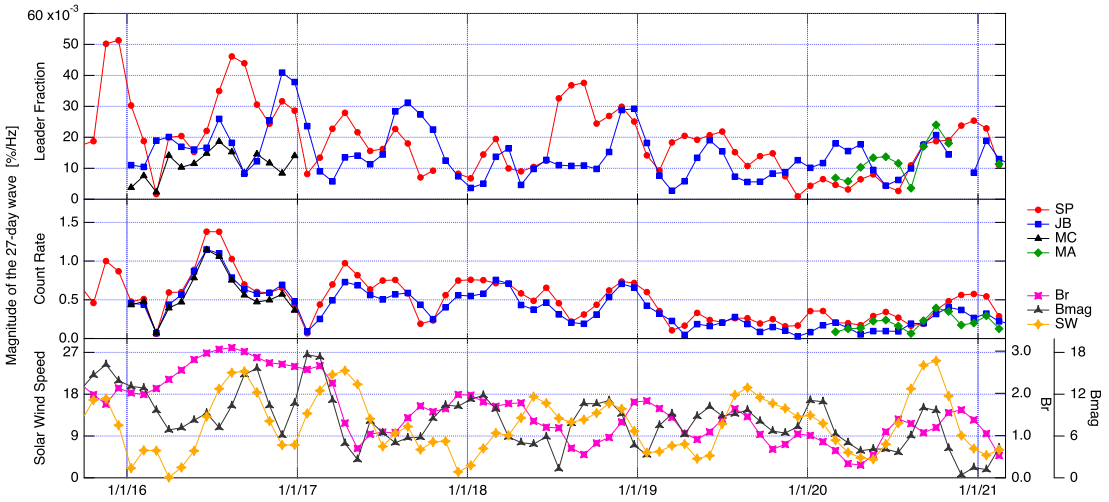

Figure 6: Magnitude of the 27-day wave from wavelet analysis of NM leader fraction (top), NM count rate (middle), and solar wind parameters (bottom), which are the SW velocity, IMF magnitude and IMF B_r component. Each point represents one Bartels rotation.

[3] R. A. Leske et al., *27-Day Modulation of Cosmic Ray Intensities During the Last Two Solar Minima*, *PoS ICRC2019*, 1105, 2019.

[4] J. W. Bieber et al., *Latitude survey observations of neutron monitor multiplicity*, *J. Geophys. Res.*, 109, A12106, 2004.

[5] R. D. Strauss et al., *The mini-neutron monitor: a new approach in neutron monitor design*, *J. Space Weather Space Clim.*, 10, 39, 2020.

[6] D. Ruffolo et al., *Monitoring Short-term Cosmic-ray Spectral Variation Using Neutron Monitor Time-delay Measurements*, *Astrophys. J.*, 817, 38, 2016.

[7] P.-S. Mangeard et al., *Dependence of the neutron monitor count rate and time delay distribution on the rigidity spectrum of primary cosmic rays*, *J. Geophys. Res. Space Physics*, 121, 11620, 2016a.

[8] C. Banglieng et al., *Tracking Cosmic-Ray Spectral Variation during 20072018 Using Neutron Monitor Time-delay Measurements*, *Astrophys. J.*, 890, 21, 2020.

[9] J. Jung et al., *Installation of Neutron Monitor at the Jang Bogo Station in Antarctica*, *J. Astron. Space Sci.*, 33(4), 345-348, (2016)a.